Published for the International Glaciological Society

THIS MANUSCRIPT HAS BEEN SUBMITTED TO THE JOURNAL OF GLACIOLOGY AND HAS NOT BEEN PEER-REVIEWED.

What can radar-based measures of subglacial hydrology tell us about basal shear stress? A case study at Thwaites Glacier, West Antarctica

Journal:	*Journal of Glaciology*
Manuscript ID	JOG-23-0099
Manuscript Type:	Article
Date Submitted by the Author:	28-Aug-2023
Complete List of Authors:	Haris, Rohaiz; Georgia Institute of Technology, School of Earth and Atmospheric Sciences Chu, Winnie; Georgia Institute of Technology, School of Earth and Atmospheric Sciences Robel, Alexander; Georgia Institute of Technology, School of Earth and Atmospheric Sciences
Keywords:	Radio-echo sounding, Subglacial processes, Ice-sheet modelling
Abstract:	Ice sheet models use observations to infer basal shear stress, but the variety of methods and datasets available has resulted in a wide range of estimates. Radar-based metrics such as reflectivity and specularity have been used to characterize subglacial hydrologic conditions that are linked to spatial variations in basal shear stress. We explore whether radar metrics can be used to inform models about basal shear stress. At Thwaites Glacier, West Antarctica, we sample basal shear stress inversions across a wide range of ice sheet models to see how the basal shear stress distribution changes in regions of varying reflectivity and specularity. Our results reveal three key findings: (1) Regions of high specularity exhibit lower mean basal shear stresses (2) Wet and bumpy regions, as characterized by high reflectivity and low specularity, exhibit higher mean basal shear stresses (3) Models disagree about what basal shear stress should be at the onset of rapid ice flow and high basal melt where reflectivity is low.

Journal of Glaciology, Vol. 00, No. 0, 0000 1

What can radar-based measures of subglacial hydrology tell us about basal shear stress? A case study at Thwaites Glacier, West Antarctica

Rohaiz HARIS,[1] Winnie CHU,[1] Alexander ROBEL[1]

[1]*School of Earth and Atmospheric Sciences, Georgia Institute of Technology*

Correspondence: Rohaiz Haris <rharis3@gatech.edu>

ABSTRACT. Ice sheet models use observations to infer basal shear stress, but the variety of methods and datasets available has resulted in a wide range of estimates. Radar-based metrics such as reflectivity and specularity have been used to characterize subglacial hydrologic conditions that are linked to spatial variations in basal shear stress. We explore whether radar metrics can be used to inform models about basal shear stress. At Thwaites Glacier, West Antarctica, we sample basal shear stress inversions across a wide range of ice sheet models to see how the basal shear stress distribution changes in regions of varying reflectivity and specularity. Our results reveal three key findings: (1) Regions of high specularity exhibit lower mean basal shear stresses (2) Wet and bumpy regions, as characterized by high reflectivity and low specularity, exhibit higher mean basal shear stresses (3) Models disagree about what basal shear stress should be at the onset of rapid ice flow and high basal melt where reflectivity is low.

1 INTRODUCTION

Glaciers and ice streams discharge ice from the interior of the Antarctic Ice Sheet to the ocean at a rate which is largely controlled by conditions at the ice-bed interface (Schoof, 2007). The influence of subglacial conditions on basal friction - and by extension on ice flow - is key to modeling the future potential evolution of the Antarctic ice sheet. Direct borehole observations over small areas of the ice sheet have been used to characterize the ice-bed interface by studying subglacial hydrologic systems (Hubbard and others, 1995) and basal friction (Pfeffer and others, 2000), but repeating these direct observations over the entire Antarctic Ice Sheet is logistically challenging. As such, alternative geophysical observational methods and forward models are typically used to analyze basal conditions over spatially extensive regions. Geophysical methods, such as seismic reflection (King, 2004) and radar sounding (Dowdeswell and Evans, 2004), are useful tools to indirectly characterize the ice-bed interface by inferring the locations of subglacial water (Chu and others, 2016), distribution of basal channels (Schroeder and others, 2013), and bed morphology (Smith, 1997). However, most individual geophysical surveys are limited to the local glacier scale and there are only a handful of repeated surveys (e.g., NASA Operation IceBridge) that cover larger areas of the Antarctic Ice Sheet.

Due to the lack of extensive physical observations on a catchment scale, basal shear stress is typically inferred from remote sensing observations (typically surface velocity and ice thickness) using control or data-assimilation methods (MacAyeal, 1993). However, the inferred basal shear stress is sensitively dependent on the details of the input dataset, the choice of the sliding law, the control method, and regularizations therein (Morlighem and others, 2010; Seroussi and others, 2013; Sergienko and Hindmarsh, 2013; Zhao and others, 2018). As a result, for the same area of an ice sheet, inversions can give a wide range of estimates for basal shear stress (Seroussi and others, 2020).

A major uncertainty in the inversion of basal shear stress is associated with the variation between sliding laws that describe the relationship between basal friction, bed roughness and rheology, and subglacial hydrology (Weertman, 1957; Lliboutry, 1968; Budd and others, 1979). The two most prominent theories, proposed by Weertman (1957) and Lliboutry (1968), describe sliding at the bed aided by bed features at various spatial scales. In Weertman (1957), sliding at the bed is dominated by two processes; regelation due to the pressure melting of ice and viscous creep around obstacles. In contrast, Lliboutry (1968) and Iken (1981) argued that cavitation plays a dominant role in influencing sliding, where the pressure from water-filled basal cavities results in small obstacles not influencing basal sliding to the extent considered in Weertman (1957). Röthlisberger (1972) also theorizes subglacial drainage channels which are maintained by melt due to the heating from turbulent flow of water, and are influenced by basal sliding due to changes in ice pressure. To make an informed decision on which sliding law is appropriate for modeling basal shear stress, it is therefore important to constrain bed characteristics, roughness, and subglacial hydrology.

Previous studies have characterized subglacial hydrology using other observable geophysical methods and investigated their relationship with basal friction. Kyrke-Smith and others (2017) utilized seismic profiles to infer acoustic impedance in order to estimate mechanical basal conditions. Comparisons between the seismic observations and high resolution basal shear stress inversions show that there is a stronger correlation between acoustic impedance and basal slipperiness or basal drag at scales longer than the ice thickness (>7 km) compared to smaller scales. Other studies have used airborne radar sounding to infer characteristics and spatial variations of subglacial hydrology using bed reflectivity (i.e., brightness of bed echo returns) and specularity content (i.e., relative contribution of specular (mirror-like reflections) signals to the total returned bed energy) (Schroeder and others, 2013; Chu and others, 2021). Das and others (2023) conducted correlation experiments and found no strong correlation between relative reflectivity and the sliding-law parameter used to control basal friction in numerical ice sheet models. These studies have suggested a potential link between the spatial distribution of subglacial hydrology and basal shear stress based on geophysical observations. In this study, we examine the statistical relationship between subglacial hydrology and basal shear stress in more detail by combining numerical ice sheet models and a high resolution radar sounding dataset from the Amundsen Sea Sector in West Antarctica. Our study site is Thwaites Glacier, located in the Amundsen Sea Embayment, which is a dominant contributor to Antarctic Ice Sheet mass loss (Pritchard and others, 2009).

2 DATA AND METHODS

2.1 Radar Sounding Observations

We use published radar bed reflectivity and specularity content observations from two airborne radar sounding studies to characterize subglacial hydrologic conditions at Thwaites Glacier (Chu and others, 2021; Schroeder and others, 2013). The radar metrics were calculated from radar sounding data measured by a High Capability Airborne Radar Sounder (HiCARS) system with a 60 MHz center frequency and 15 MHz bandwidth (Peters and others, 2007). The data was collected as part of a campaign that conducted airborne radar sounding surveys of the Amundsen Sea Embayment during the 2004/2005 austral field season (Holt and others, 2006; Vaughan and others, 2006).

Bed reflectivity describes the brightness of returned bed echoes and is mostly influenced by the difference in dielectric permittivity between two materials (Peters, 2005). A vertical transition between ice and liquid freshwater results in a 10 - 15 dB increase in reflectivity relative to the surrounding ice-bed interface

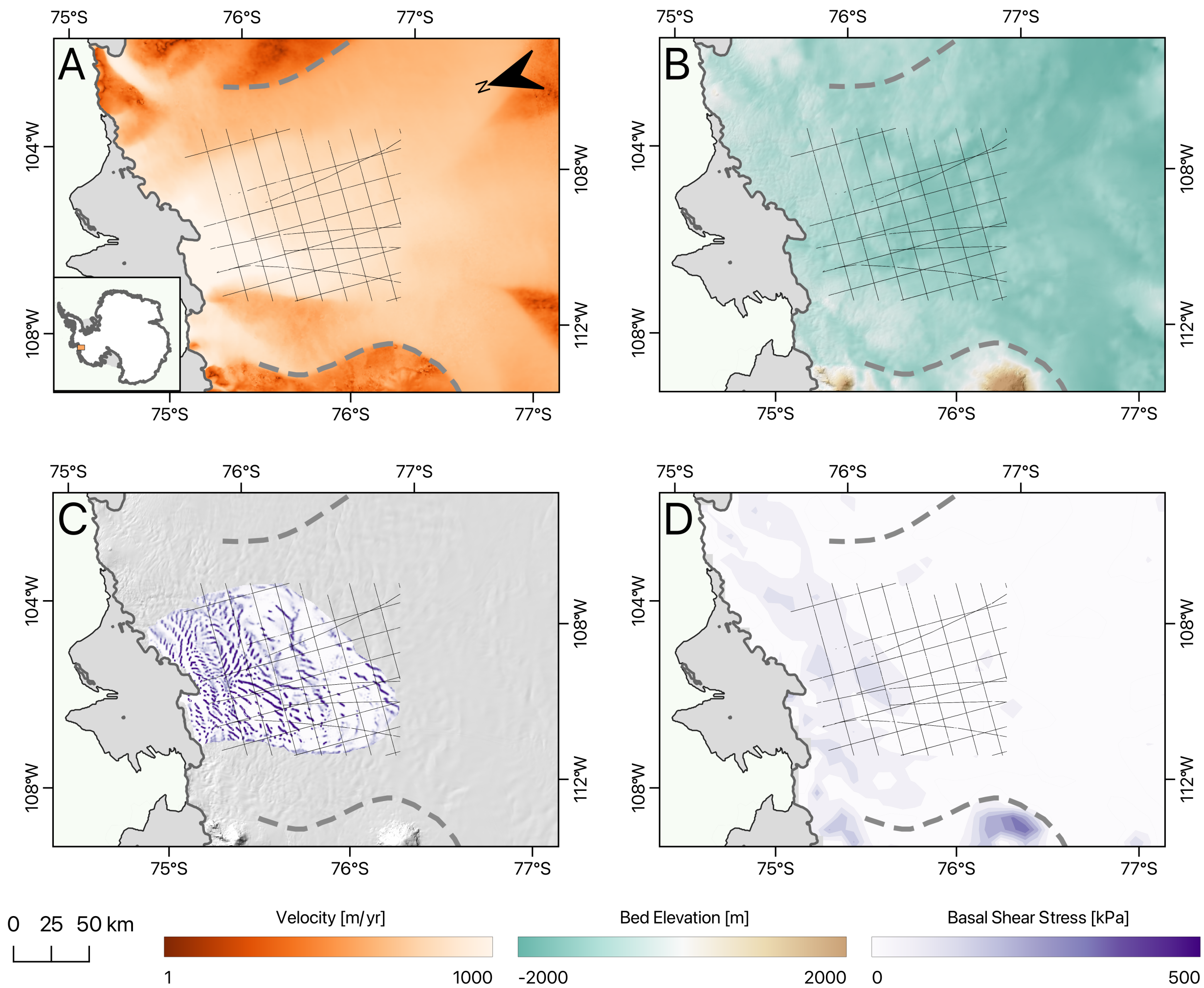

Fig. 1. Site Map indicating radar flight tracks (black line) (Chu and others, 2021), shear margin (dotted grey line) (Schroeder and others, 2013), with (A) MEaSUREs ice velocity (Rignot and University Of California Irvine, 2017; Mouginot and others, 2017), (B) BedMachine v3 bed topography (Morlighem and others, 2020; Morlighem, 2022) & REMA hillshade (Howat and others, 2022), (C) basal shear stress inversion from Sergienko and Hindmarsh (2013) and (D) JPL1 ISSM basal shear stress inversion (Seroussi and others, 2020)

(Peters, 2005; Chu and others, 2016; Young and others, 2016). We use relative reflectivity from Chu and others (2021) which captures spatial variations within a study site as opposed to absolute reflectivity which is influenced by many unknown parameters specific to the site (Peters and others, 2007; Chu and others, 2021).

Specularity is a measure of the angular distribution of the bed echo power, with values ranging from 0 to 1. Differences in ice-bedrock interface geometry produce unique scattering signatures that can be used to characterize interface roughness and subglacial hydrology. Thus, specularity content is typically interpreted to indicate a change in interface roughness (Schroeder and others, 2013). Smooth interfaces will return sharp mirror-like reflections. This results in higher specularity values (>0.3) that are thought to be indicative of a smooth interface such as a region of low bed roughness or subglacial lakes with flat surfaces. Conversely, diffuse interfaces will scatter energy in all directions and have a low specularity content (<0.3) (Schroeder and others, 2013; Young and others, 2016; Chu and others, 2021). The goal of our study is not to definitively distinguish between the influence of bed roughness versus material contrast on bed reflectivity or specularity content; but to explore whether these radar metrics correspond to any changes in basal shear stress suggested by ice sheet models. This is also the reason why we choose to combine both relative reflectivity and specularity content (each sensitive to a different degree to the presence of subglacial water or changes in bed roughness) to provide a more comprehensive interpretation of basal conditions at Thwaites Glacier.

2.2 Model-Inferred Basal Friction

Basal shear stress on a continental scale is typically inferred from inverse methods in ice sheet models (Sergienko and others, 2008; MacAyeal, 1992; Pattyn and others, 2017) using large-scale remote sensing measurements such as ice velocity, surface elevation and ice thickness. We use previously published basal shear stress inversions from a subset of Antarctic ice sheet model simulations included in the most recent Ice Sheet Model Intercomparison project (Seroussi and others, 2020). The subset of models include: AWI PISM1, JPL1 ISSM, PIK PISM1, UCIJPL ISSM, UTAS ElmerIce, VUB AISMPALEO, DOE MALI, NCAR CISM. Each modeling group participating in ISMIP6 uses their own inversion method to initialize the basal shear stress field, which is then held constant for the transient simulations of future ice sheet behavior which are the focus of the inter-comparison exercise. Thus, this ensemble of inversions is a representative sampling of the best estimates of basal shear stress which are used to predict future ice sheet behavior. We have also added the inversion from Sergienko and Hindmarsh (2013) which includes some finer resolution (kilometer-scale) features not present in ISMIP6 inversions. Most inversions examined in this study use some variation of the control method described in MacAyeal (1993) to minimize the misfit between the observed and modeled ice sheet surface velocities (Morlighem and others, 2010). The control method uses a cost function and subsequent optimizations to reduce the error between a forward model's output and observations such as surface velocity or topography (Ranganathan and others, 2021). Different modeling groups use different variations of the cost function in MacAyeal (1993) and apply their own regularizations and optimizations as well. For example, some cost functions may prioritize reducing the velocity misfit in slow moving regions (Morlighem and others, 2010), while other cost functions may not consider velocity direction and only reduce misfit in the magnitude of velocities (Zhao and others, 2018). Other models use transient spin-up methods (Schoof, 2006; Pollard and DeConto, 2012) that assimilate observations to nudge the output to minimize the mismatch between modeled and observed data. Ultimately, such differences in inversion methodology and input data lead to a wide range of predicted basal shear stress among the models considered here. Since direct observations of basal shear stress are sparse (or absent entirely in some regions, including the region we consider in this study), inversions are not validated against observations. Thus, we instead consider a representative sample of nine inversions and analyze where these inversions agree and disagree with each other in terms of their statistical relationship to radar sounding metrics.

2.3 Statistical Methods for Comparison of Radar Observations and Modeled Data

Due to varying spatial resolutions of the basal shear stress inversions used in this study and the higher resolution of radar data, all inversions of basal shear stress were interpolated onto the radar flight track coordinates. The nearest neighbor basal shear stress value to each coordinate on the radar track was mapped onto that point unchanged. If that exact basal shear stress value was absent, the next closest basal shear stress value within a 5 km radius was used.

Prior studies (e.g., Kyrke-Smith and others (2017); Das and others (2023)) have attempted to quantify the relationship between measures of subglacial hydrology and basal shear stress using regression methods and generally failed to do so except at spatial scales larger than 7 km. The same is true for the radar and basal shear stress data used here. We first examined the linear regression between the modeled basal shear stress and the two radar indices, relative reflectivity and specularity respectively. On a basin scale, the largest Pearson correlation coefficient observed across all models was 0.419 between VUB AISMPALEO basal shear stress and relative reflectivity. There is no significant relationship that can be deduced using regression techniques between basal shear stress and radar metrics for subglacial hydrology at any length scale. Instead, we use sampling statistics to determine if radar metrics can be used to classify regions with statistically significant variations in basal shear stress. After sub-sampling the model-based values of basal shear stress using every possible permutation of reflectivity and specularity thresholds, we analyze how the mean basal shear stress changes across different inversions and different radar metric thresholds. Basal shear stress samples with less than 100 values are not considered to ensure that any changes in the basal shear stress distribution are not due to individual outliers within small sample sizes. We also identify where regions of significant deviation in mean basal shear stress occur and how they relate to other variables such as surface ice velocity and bed topography.

Finally, we used two-sample Kolmogorov-Smirnov testing to verify whether sub-sampling basal shear stress on the basis of radar data produces a statistically significant difference in the sub-sampled basal shear stress distribution compared to randomly sampling the same number of points from the entire basal shear stress dataset. The two-sample Kolmogorov-Smirnov test (henceforth referred to as KS test) is a hypothesis test that evaluates the difference in cumulative distribution functions (CDFs) of two datasets and can be used to evaluate whether both samples share the same continuous distribution (Dimitrova and others, 2020)). In KS testing, our null hypothesis is that the sub-sampled data and the overall basal shear stress data share the same distribution, which would indicate that reflectivity and specularity are not useful tools for discriminating regions with different basal shear stress. Rejecting the null hypothesis for a particular reflectivity and specularity threshold is a useful way to identify regions with different basal shear stresses. Samples that make up 70 percent or more of the inversion dataset are not considered as these are likely to be representative of the entire dataset and have well known issues when inferring the difference between distributions. The KS test is overly sensitive for large sample sizes and detects a statistically significant difference between the sub-sampled data and the complete basal shear stress dataset even if the actual difference is negligible (Sullivan and Feinn, 2012; Larson, 2018). Due to this sensitivity to sample size, we perform the KS test on data sub-sampled on the basis of reflectivity and specularity and a random sample of the same size to avoid a Type I error which occurs when the null hypothesis is rejected incorrectly.

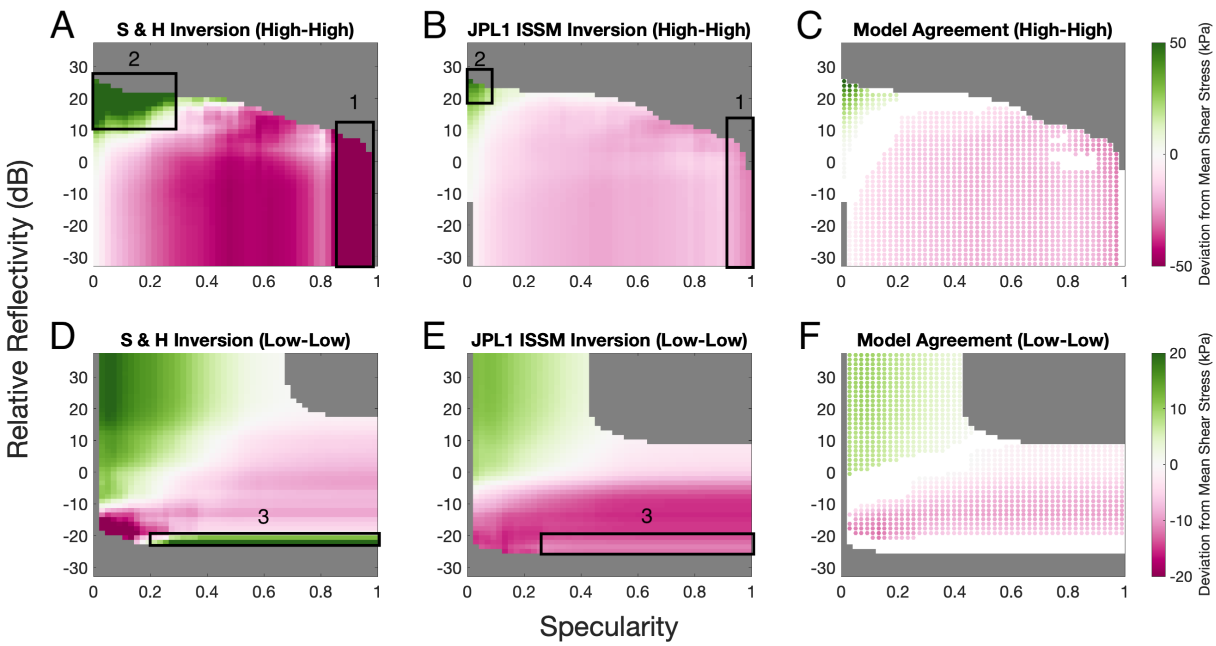

Fig. 2. 2A and 2B show the high-high plots for the inversion from Sergienko and Hindmarsh (2013) and JPL1 ISSM inversion (Seroussi and others, 2020) respectively. Thresholds of specularity > X and relative reflectivity > Y are applied for sub-sampling. 2D and 2E show the low-low plots for the inversion from Sergienko and Hindmarsh (2013) and JPL1 ISSM inversion respectively. Thresholds of specularity < X and relative reflectivity < Y are applied for sub-sampling. The colormap for 2A, 2B, 2D & 2E represent the deviation in mean basal shear stress of the sample from the overall basal shear stress distribution. Figures 2C and 2F show where seven or more inversions agreed on the sign of deviation from mean basal shear stress on the high-high plot and low-low plot respectively. Colored markers indicate the inter-model mean of the deviation in mean basal shear stress for that relative reflectivity and specularity threshold.

3 RESULTS

We investigate whether using reflectivity and specularity thresholds as sampling criteria produce statistically significant differences in basal shear stress across a range of model inversion products. The results from sub-sampling are illustrated in Figure 2 in a 50x50 grid, where each grid square reflects the deviation in mean basal shear stress for a sub-sample based on either maximum or minimum thresholds of specularity and reflectivity, with respect to the mean basal shear stress over all radar flight lines. Though we have calculated these basal shear stress deviations for all nine inversions considered in this study, Figures 2A and 2D plot results for the inversion of Sergienko and Hindmarsh (2013) and Figures 2B and 2E plot results of the JPL1 ISSM inversion from ISMIP6 (Seroussi and others, 2020). In Figures 2A and 2B (referred to hereafter as "high-high" plots), we apply a combination of reflectivity and specularity thresholds to sub-sample each inversion such that specularity is greater than X and relative reflectivity is greater than Y where X and Y correspond to values on the x-axis and the y-axis. Conversely in Figures 2D and 2E (referred to as "low-low" plots), the combination of reflectivity and specularity thresholds applied are specularity less than X and relative reflectivity less than Y.

We identify three regimes in Figure 2 where sub-sampling with reflectivity and specularity thresholds lead to a substantial and coherent deviation in mean basal shear stress across most (or all nine) inversion products as verified by KS testing. While the range of spatial variation in basal shear stress differs between the models, the sign of deviation in mean basal shear stress is consistent across models for Regime 1 and Regime 2. Regime 1 occurs in areas where specularity is > 0.85, and there is a significant decrease in mean basal shear stress from 1 kPa up to 81 kPa depending on the inversion product. Regime 2 occurs in areas where relative reflectivity is between 20 dB and 35 dB and specularity is typically < 0.1 (though the exact reflectivity and specularity boundaries vary depending on the inversion). In this bright but diffuse bed environment, there is a significant increase in mean basal shear stress from 3 kPa up to 160 kPa depending on the inversion product. Finally, regime 3 occurs in dim bed areas where relative reflectivity is $<$ -20 dB where there is a significant deviation in mean basal shear stress across all inversions. However, inversions disagree on the sign of this deviation in mean basal shear stress. Three inversions indicate a significant increase in mean basal shear stress from 2 kPa up to 88 kPa depending to the inversion product. Conversely, the remaining six inversions indicate a significant decrease in mean basal shear stress from 7 kPa up to 17 kPa depending on the inversion product.

4 DISCUSSION

In regions of high specularity (Regime 1 identified in Figure 2A and 2B), a lower mean basal shear stress was observed across all inversions. Reflected radar energy from smooth ice-bedrock interfaces is specular due to minimal scattering (Schroeder and others, 2015; Young and others, 2016). Regions of high specularity have also been proposed as the location of broad canals incised into the subglacial till below Thwaites Glacier (Schroeder and others, 2013) or spatially continuous subglacial water sheets, which are both thought to reduce basal friction over large regions (Walder and Fowler, 1994; Creyts and Schoof, 2009).

Regions of low specularity and high reflectivity (Regime 2 identified in Figure 2A and 2B) show a higher mean basal shear stress across all inversions. The combination of low specularity and high reflectivity is thought to be indicative of wet regions with a rough ice surface, which would be seen in concentrated Röthlisberger channels of water incised upward into the basal glacier ice (Schroeder and others, 2013). Such concentrated channels reduce the water flow through extensive distributed drainage systems, and so are thought to increase basal friction on average (Schoof, 2010), which is consistent with our findings of higher mean basal shear stress in these regions.

Regions of high specularity and lower mean basal shear stress are located in the upstream reaches of the Thwaites catchment, while regions of low specularity, high reflectivity and higher mean basal shear stress are located in the downstream reaches of the Thwaites catchment. It has been theorized that the transition from a distributed to channelized water system at Thwaites Glacier is accompanied by an increase in basal shear stress (Schroeder and others, 2013). Our results are consistent with this prior hypothesis where we see an increase in mean basal shear stress from Regime 1 to Regime 2. We independently identify this transition in Figure 3A and 3C which is consistent with the transition identified in Schroeder and others (2013).

Regions of low reflectivity (Regime 3 identified in Figure 2D and 2E) are indicative of a dry bed and show strong deviations from mean basal shear stress over the whole Thwaites study within particular inversions, but the sign of the deviation is not consistent between inversions. Three inversions considered in this study have high basal shear stress in low reflectivity regions, while the other six inversions have low basal shear stress. This region of disagreement between inversions is occurring at the onset of rapid ice flow and high basal melt (i.e., where ice velocity is approximately 250 m yr^{-1} in Fig 3B and 3D denoted by the purple contour). The location of onset of rapid flow is known to vary widely between models due to

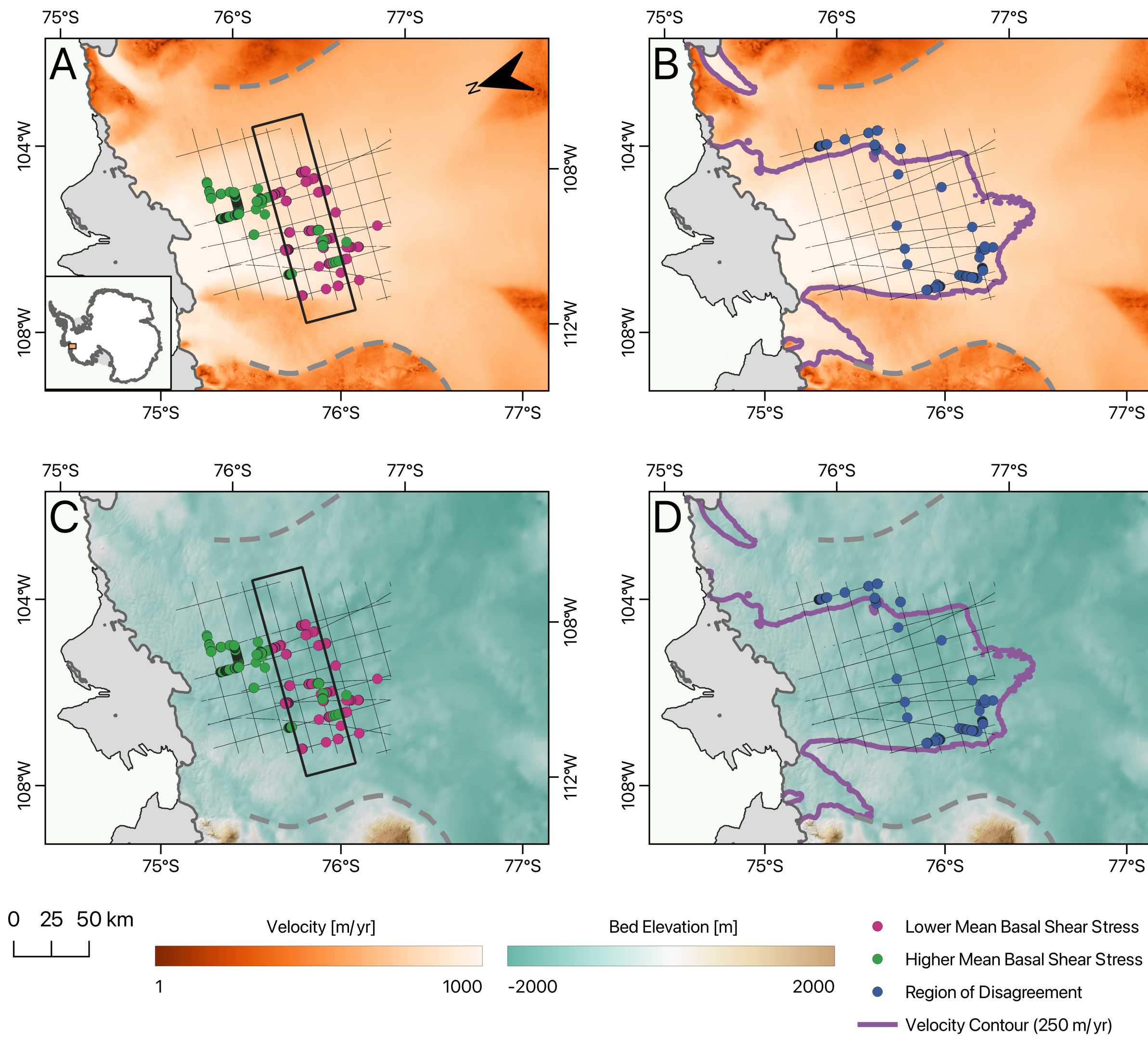

Fig. 3. Spatial plot to observe variations in regions of significant deviation in mean basal shear stress. (A) Region 1 where there is high specularity and Region 2 where there is high reflectivity and low specularity with MEaSUREs ice velocity (Rignot and University Of California Irvine, 2017; Mouginot and others, 2017), (B) Region 3 where there is low reflectivity with MEaSUREs ice velocity. (C) Region 1 and Region 2 with BedMachine v3 bed topography (Morlighem and others, 2020; Morlighem, 2022) and REMA hillshade (Howat and others, 2022), (D) Region 3 with BedMachine v3 bed topography and REMA hillshade. The box in (A) and (C) represents our identified transition from a distributed to channelized system accompanied by an increase in mean basal shear stress. The purple contour line in (B) and (D) represents where ice velocity is 250 m yr^{-1}.

generally inadequate treatments of the thermo-mechanical conditions in ice stream onset regions (Mantelli and others, 2019; Mantelli and Schoof, 2019). Models taking part in ISMIP6 may also differ on the location of streaming ice flow due to differing horizontal resolution or ice flow approximations (Payne and others, 2000; Hindmarsh, 2009).

Other studies have also investigated the correspondence between indirect geophysical measures of subglacial hydrology to basal shear stress. Das and others (2023) calculated correlations between radar reflectivity and sliding law parameter (representative of basal friction) for 3 models and were unable to find a strong correlation. Kyrke-Smith and others (2017) found that there may not be a discernible relationship between subglacial hydrology and basal shear stress at short length scales (below 7 km), as they observed no correlation between acoustic impedance and basal shear stress within seismic profiles. However, a stronger correlation was observed when values were averaged over an ice thickness scale and distinct profiles were compared. Our study is consistent with the conclusions of Das and others (2023) and Kyrke-Smith and others (2017). We were unable to find a statistically significant relationship between basal shear stress and reflectivity or specularity using regression techniques across radar profiles. However, we do identify at least two useful radar metric thresholds for identifying regions of substantial deviations in basal shear stress which are statistically distinct from random sampling of basal shear stress data. This novel approach has also revealed that regions of low reflectivity indicative of a dry bed consistently occur at the zone of Thwaites Glacier where ice starts to flow fast. However, basal shear stress inversions tend to disagree about the basal shear stress in this region, thus requiring better constraints to be able to model ice flow in this region more accurately. The relationship between subglacial hydrology and basal shear stress may not be apparent at short length scales which are filtered out by ice sheet dynamics (Raymond and Gudmundsson, 2005) and may not be apparent in surface velocity which is the main constraint for basal shear stress inversions. Many sliding laws quantify the relationships between ice velocity, basal shear stress and basal water pressure. However, other factors may also play a role in controlling basal sliding, and radar sounding provides independent constraints on those factors that may not be captured by current inversion methods.

5 CONCLUSION

Different ice sheet models use different methods and datasets to compute sliding law parameters, resulting in a wide range of estimates for basal shear stress. In this study, we have shown that radar sounding can be used to identify regions of low reflectivity characterized by a unique radar signature where models produce widely differing constraints on basal shear stress. Presently, ice velocity and thickness are the main constraints for inversions. Radar sounding can potentially provide an independent constraint on subglacial properties that have been previously theorized to influence basal shear stress through subglacial hydrology. Such threshold constraints could be incorporated into control methods using inequality constraints, for which there are existing optimization methods (Bryson and others, 1963). However, reflectivity and specularity are affected by parameters other than subglacial hydrologic systems such as properties of subglacial material (till vs bedrock, etc.). While results from this study have shown that radar can be useful in providing constraints on factors not yet captured by inversions, further work on the theory of basal sliding and data assimilation into ice sheet models is required before radar sounding metrics can be used directly to inform ice-flow models on subglacial conditions.

6 DATA AVAILABILITY

The code used in this study can be found on Github (https://github.com/rohaizharis/inversion_radar2022). The bed reflectivity data is from Chu and others (2021) and specularity data is from Schroeder and others (2013). The inversions used in this study are from Sergienko and Hindmarsh (2013) and Seroussi and others (2020). The interpolated data for use with the code can be found on Zenodo (https://doi.org/10.5281/zenodo.8290523). The surface ice velocity from MEaSUREs (Rignot and University Of California Irvine, 2017; Mouginot and others, 2017), bed topography from BedMachine v3 (Morlighem and others, 2020; Morlighem, 2022), surface elevation hillshade from REMA (Howat and others, 2022), can be found online.

7 ACKNOWLEDGMENTS

All authors were supported using startup funds from Georgia Institute of Technology. We would like to thank Vincent Verjans, Ziad Rashed, Angelo Tarzona and Kiera Tran for their feedback on the figures shown.

REFERENCES

Bryson AE, Denham WF and Dreyfus SE (1963) Optimal programming problems with inequality constraints. *AIAA Journal*, **1**(11), 2544–2550, ISSN 0001-1452, 1533-385X (doi: 10.2514/3.2107)

Budd WF, Keage PL and Blundy NA (1979) Empirical Studies of Ice Sliding. *Journal of Glaciology*, **23**(89), 157–170, ISSN 0022-1430, 1727-5652 (doi: 10.3189/S0022143000029804)

Chu W, Schroeder DM, Seroussi H, Creyts TT, Palmer SJ and Bell RE (2016) Extensive winter subglacial water storage beneath the Greenland Ice Sheet. *Geophysical Research Letters*, **43**(24), ISSN 0094-8276, 1944-8007 (doi: 10.1002/2016GL071538)

Chu W, Hilger AM, Culberg R, Schroeder DM, Jordan TM, Seroussi H, Young DA, Blankenship DD and Vaughan DG (2021) Multisystem Synthesis of Radar Sounding Observations of the Amundsen Sea Sector From the 2004–2005 Field Season. *Journal of Geophysical Research: Earth Surface*, **126**(10), ISSN 2169-9003, 2169-9011 (doi: 10.1029/2021JF006296)

Creyts TT and Schoof CG (2009) Drainage through subglacial water sheets. *Journal of Geophysical Research*, **114**(F4), F04008, ISSN 0148-0227 (doi: 10.1029/2008JF001215)

Das I, Morlighem M, Barnes J, Gudmundsson GH, Goldberg D and Dias Dos Santos T (2023) In the Quest of a Parametric Relation Between Ice Sheet Model Inferred Weertman's Sliding-Law Parameter and Airborne Radar-Derived Basal Reflectivity Underneath Thwaites Glacier, Antarctica. *Geophysical Research Letters*, **50**(10), e2022GL098910, ISSN 0094-8276, 1944-8007 (doi: 10.1029/2022GL098910)

Dimitrova DS, Kaishev VK and Tan S (2020) Computing the Kolmogorov-Smirnov Distribution When the Underlying CDF is Purely Discrete, Mixed, or Continuous. *Journal of Statistical Software*, **95**(10), ISSN 1548-7660 (doi: 10.18637/jss.v095.i10)

Dowdeswell JA and Evans S (2004) Investigations of the form and flow of ice sheets and glaciers using radio-echo sounding. *Reports on Progress in Physics*, **67**(10), 1821–1861, ISSN 0034-4885, 1361-6633 (doi: 10.1088/0034-4885/67/10/R03)

Hindmarsh RCA (2009) Consistent generation of ice-streams via thermo-viscous instabilities modulated by membrane stresses. *Geophysical Research Letters*, **36**(6), L06502, ISSN 0094-8276 (doi: 10.1029/2008GL036877)

Holt JW, Blankenship DD, Morse DL, Young DA, Peters ME, Kempf SD, Richter TG, Vaughan DG and Corr HFJ (2006) New boundary conditions for the West Antarctic Ice Sheet: Subglacial topography of the Thwaites and Smith glacier catchments. *Geophysical Research Letters*, **33**(9), L09502, ISSN 0094-8276 (doi: 10.1029/2005GL025561)

Howat I, Porter C, Noh MJ, Husby E, Khuvis S, Danish E, Tomko K, Gardiner J, Negrete A, Yadav B, Klassen J, Kelleher C, Cloutier M, Bakker J, Enos J, Arnold G, Bauer G and Morin P (2022) The Reference Elevation Model of Antarctica - Mosaics, Version 2 (doi: 10.7910/DVN/EBW8UC)

Hubbard BP, Sharp MJ, Willis IC, Nielsen MK and Smart CC (1995) Borehole water-level variations and the structure of the subglacial hydrological system of Haut Glacier d'Arolla, Valais, Switzerland. *Journal of Glaciology*, **41**(139), 572–583, ISSN 0022-1430, 1727-5652 (doi: 10.3189/S0022143000034894)

Iken A (1981) The Effect of the Subglacial Water Pressure on the Sliding Velocity of a Glacier in an Idealized Numerical Model. *Journal of Glaciology*, **27**(97), 407–421, ISSN 0022-1430, 1727-5652 (doi: 10.3189/S0022143000011448)

King EC (2004) Seismic evidence for a water-filled canal in deforming till beneath Rutford Ice Stream, West Antarctica. *Geophysical Research Letters*, **31**(20), L20401, ISSN 0094-8276 (doi: 10.1029/2004GL020379)

Kyrke-Smith TM, Gudmundsson GH and Farrell PE (2017) Can Seismic Observations of Bed Conditions on Ice Streams Help Constrain Parameters in Ice Flow Models?: COMPARISON OF INVERSIONS AND SEISMICS. *Journal of Geophysical Research: Earth Surface*, **122**(11), 2269–2282, ISSN 21699003 (doi: 10.1002/2017JF004373)

Larson LG (2018) *Investigating Statistical vs. Practical Significance of the Kolmogorov-Smirnov Two-Sample Test Using Power Simulations and Resampling Procedures*. Ph.D. thesis

Lliboutry L (1968) General Theory of Subglacial Cavitation and Sliding of Temperate Glaciers. *Journal of Glaciology*, **7**(49), 21–58, ISSN 0022-1430, 1727-5652 (doi: 10.3189/S0022143000020396)

MacAyeal DR (1992) The basal stress distribution of Ice Stream E, Antarctica, inferred by control methods. *Journal of Geophysical Research*, **97**(B1), 595, ISSN 0148-0227 (doi: 10.1029/91JB02454)

MacAyeal DR (1993) A tutorial on the use of control methods in ice-sheet modeling. *Journal of Glaciology*, **39**(131), 91–98, ISSN 0022-1430, 1727-5652 (doi: 10.3189/S0022143000015744)

Mantelli E and Schoof C (2019) Ice sheet flow with thermally activated sliding. Part 2: the stability of subtemperate regions. *Proceedings of the Royal Society A: Mathematical, Physical and Engineering Sciences*, **475**(2231), 20190411, ISSN 1364-5021, 1471-2946 (doi: 10.1098/rspa.2019.0411)

Mantelli E, Haseloff M and Schoof C (2019) Ice sheet flow with thermally activated sliding. Part 1: the role of advection. *Proceedings of the Royal Society A: Mathematical, Physical and Engineering Sciences*, **475**(2230), 20190410, ISSN 1364-5021, 1471-2946 (doi: 10.1098/rspa.2019.0410)

Morlighem M (2022) MEaSUREs BedMachine Antarctica, Version 3 (doi: 10.5067/FPSU0V1MWUB6)

Morlighem M, Rignot E, Seroussi H, Larour E, Ben Dhia H and Aubry D (2010) Spatial patterns of basal drag inferred using control methods from a full-Stokes and simpler models for Pine Island Glacier, West Antarctica: SPATIAL PATTERNS OF BASAL DRAG. *Geophysical Research Letters*, **37**(14), n/a–n/a, ISSN 00948276 (doi: 10.1029/2010GL043853)

Morlighem M, Rignot E, Binder T, Blankenship D, Drews R, Eagles G, Eisen O, Ferraccioli F, Forsberg R, Fretwell P, Goel V, Greenbaum JS, Gudmundsson H, Guo J, Helm V, Hofstede C, Howat I, Humbert A, Jokat W, Karlsson NB, Lee WS, Matsuoka K, Millan R, Mouginot J, Paden J, Pattyn F, Roberts J, Rosier S, Ruppel A, Seroussi H, Smith EC, Steinhage D, Sun B, Broeke MRVD, Ommen TDV, Wessem MV and Young DA (2020) Deep glacial troughs and stabilizing ridges unveiled beneath the margins of the Antarctic ice sheet. *Nature Geoscience*, **13**(2), 132–137, ISSN 1752-0894, 1752-0908 (doi: 10.1038/s41561-019-0510-8)

Mouginot J, Rignot E, Scheuchl B and Millan R (2017) Comprehensive Annual Ice Sheet Velocity Mapping Using Landsat-8, Sentinel-1, and RADARSAT-2 Data. *Remote Sensing*, **9**(4), 364, ISSN 2072-4292 (doi: 10.3390/rs9040364)

Pattyn F, Favier L, Sun S and Durand G (2017) Progress in Numerical Modeling of Antarctic Ice-Sheet Dynamics. *Current Climate Change Reports*, **3**(3), 174–184, ISSN 2198-6061 (doi: 10.1007/s40641-017-0069-7)

Payne AJ, Huybrechts P, Abe-Ouchi A, Calov R, Fastook JL, Greve R, Marshall SJ, Marsiat I, Ritz C, Tarasov L and Thomassen MPA (2000) Results from the EISMINT model intercomparison: the effects of thermomechanical coupling. *Journal of Glaciology*, **46**(153), 227–238, ISSN 0022-1430, 1727-5652 (doi: 10.3189/172756500781832891)

Peters M, Blankenship D, Carter S, Kempf S, Young D and Holt J (2007) Along-Track Focusing of Airborne Radar Sounding Data From West Antarctica for Improving Basal Reflection Analysis and Layer Detection. *IEEE Transactions on Geoscience and Remote Sensing*, **45**(9), 2725–2736, ISSN 0196-2892 (doi: 10.1109/TGRS.2007.897416)

Peters ME (2005) Analysis techniques for coherent airborne radar sounding: Application to West Antarctic ice streams. *Journal of Geophysical Research*, **110**(B6), B06303, ISSN 0148-0227 (doi: 10.1029/2004JB003222)

Pfeffer WT, Humphrey NF, Amadei B, Harper J and Wegmann J (2000) In situ stress tensor measured in an Alaskan glacier. *Annals of Glaciology*, **31**, 229–235, ISSN 0260-3055, 1727-5644 (doi: 10.3189/172756400781820354)

Pollard D and DeConto RM (2012) A simple inverse method for the distribution of basal sliding coefficients under ice sheets, applied to Antarctica. *The Cryosphere*, **6**(5), 953–971, ISSN 1994-0424 (doi: 10.5194/tc-6-953-2012)

Pritchard HD, Arthern RJ, Vaughan DG and Edwards LA (2009) Extensive dynamic thinning on the margins of the Greenland and Antarctic ice sheets. *Nature*, **461**(7266), 971–975, ISSN 0028-0836, 1476-4687 (doi: 10.1038/nature08471)

Ranganathan M, Minchew B, Meyer CR and Gudmundsson GH (2021) A new approach to inferring basal drag and ice rheology in ice streams, with applications to West Antarctic Ice Streams. *Journal of Glaciology*, **67**(262), 229–242, ISSN 0022-1430, 1727-5652 (doi: 10.1017/jog.2020.95)

Raymond MJ and Gudmundsson GH (2005) On the relationship between surface and basal properties on glaciers, ice sheets, and ice streams. *Journal of Geophysical Research*, **110**(B8), B08411, ISSN 0148-0227 (doi: 10.1029/2005JB003681)

Rignot E and University Of California Irvine (2017) MEaSUREs Annual Antarctic Ice Velocity Maps, 2006-2017, Version 1 (doi: 10.5067/9T4EPQXTJYW9)

Röthlisberger H (1972) Water Pressure in Intra- and Subglacial Channels. *Journal of Glaciology*, **11**(62), 177–203, ISSN 0022-1430, 1727-5652 (doi: 10.3189/S0022143000022188)

Schoof C (2006) Variational methods for glacier flow over plastic till. *Journal of Fluid Mechanics*, **555**, 299, ISSN 0022-1120, 1469-7645 (doi: 10.1017/S0022112006009104)

Schoof C (2007) Ice sheet grounding line dynamics: Steady states, stability, and hysteresis. *Journal of Geophysical Research*, **112**(F3), F03S28, ISSN 0148-0227 (doi: 10.1029/2006JF000664)

Schoof C (2010) Ice-sheet acceleration driven by melt supply variability. *Nature*, **468**(7325), 803–806, ISSN 0028-0836, 1476-4687 (doi: 10.1038/nature09618)

Schroeder DM, Blankenship DD and Young DA (2013) Evidence for a water system transition beneath Thwaites Glacier, West Antarctica. *Proceedings of the National Academy of Sciences*, **110**(30), 12225–12228, ISSN 0027-8424, 1091-6490 (doi: 10.1073/pnas.1302828110)

Schroeder DM, Blankenship DD, Raney RK and Grima C (2015) Estimating Subglacial Water Geometry Using Radar Bed Echo Specularity: Application to Thwaites Glacier, West Antarctica. *IEEE Geoscience and Remote Sensing Letters*, **12**(3), 443–447, ISSN 1545-598X, 1558-0571 (doi: 10.1109/LGRS.2014.2337878)

Sergienko OV and Hindmarsh RCA (2013) Regular Patterns in Frictional Resistance of Ice-Stream Beds Seen by Surface Data Inversion. *Science*, **342**(6162), 1086–1089, ISSN 0036-8075, 1095-9203 (doi: 10.1126/science.1243903)

Sergienko OV, Bindschadler RA, Vornberger PL and MacAyeal DR (2008) Ice stream basal conditions from block-wise surface data inversion and simple regression models of ice stream flow: Application to Bindschadler Ice Stream. *Journal of Geophysical Research*, **113**(F4), F04010, ISSN 0148-0227 (doi: 10.1029/2008JF001004)

Seroussi H, Morlighem M, Rignot E, Khazendar A, Larour E and Mouginot J (2013) Dependence of century-scale projections of the Greenland ice sheet on its thermal regime. *Journal of Glaciology*, **59**(218), 1024–1034, ISSN 0022-1430, 1727-5652 (doi: 10.3189/2013JoG13J054)

Seroussi H, Nowicki S, Payne AJ, Goelzer H, Lipscomb WH, Abe-Ouchi A, Agosta C, Albrecht T, Asay-Davis X, Barthel A, Calov R, Cullather R, Dumas C, Galton-Fenzi BK, Gladstone R, Golledge NR, Gregory JM, Greve R, Hattermann T, Hoffman MJ, Humbert A, Huybrechts P, Jourdain NC, Kleiner T, Larour E, Leguy GR, Lowry DP, Little CM, Morlighem M, Pattyn F, Pelle T, Price SF, Quiquet A, Reese R, Schlegel NJ, Shepherd A, Simon E, Smith RS, Straneo F, Sun S, Trusel LD, Van Breedam J, van de Wal RSW, Winkelmann R, Zhao C, Zhang T and Zwinger T (2020) ISMIP6 Antarctica: a multi-model ensemble of the Antarctic ice sheet evolution over the 21st century. *The Cryosphere*, **14**(9), 3033–3070, ISSN 1994-0424 (doi: 10.5194/tc-14-3033-2020)

Smith AM (1997) Basal conditions on Rutford Ice Stream, West Antarctica, from seismic observations. *Journal of Geophysical Research: Solid Earth*, **102**(B1), 543–552, ISSN 01480227 (doi: 10.1029/96JB02933)

Sullivan GM and Feinn R (2012) Using Effect Size—or Why the P Value Is Not Enough. *Journal of Graduate Medical Education*, **4**(3), 279–282, ISSN 1949-8357, 1949-8349 (doi: 10.4300/JGME-D-12-00156.1)

Vaughan DG, Corr HFJ, Ferraccioli F, Frearson N, O'Hare A, Mach D, Holt JW, Blankenship DD, Morse DL and Young DA (2006) New boundary conditions for the West Antarctic ice sheet: Subglacial topography beneath Pine Island Glacier. *Geophysical Research Letters*, **33**(9), L09501, ISSN 0094-8276 (doi: 10.1029/2005GL025588)

Walder JS and Fowler A (1994) Channelized subglacial drainage over a deformable bed. *Journal of Glaciology*, **40**(134), 3–15, ISSN 0022-1430, 1727-5652 (doi: 10.3189/S0022143000003750)

Weertman J (1957) On the Sliding of Glaciers. *Journal of Glaciology*, **3**(21), 33–38, ISSN 0022-1430, 1727-5652 (doi: 10.3189/S0022143000024709)

Young DA, Schroeder DM, Blankenship DD, Kempf SD and Quartini E (2016) The distribution of basal water between Antarctic subglacial lakes from radar sounding. *Philosophical Transactions of the Royal Society A: Mathematical, Physical and Engineering Sciences*, **374**(2059), 20140297 (doi: 10.1098/rsta.2014.0297)

Zhao C, Gladstone RM, Warner RC, King MA, Zwinger T and Morlighem M (2018) Basal friction of Fleming Glacier, Antarctica – Part 1: Sensitivity of inversion to temperature and bedrock uncertainty. *The Cryosphere*, **12**(8), 2637–2652, ISSN 1994-0424 (doi: 10.5194/tc-12-2637-2018)